

ARTICLE OPEN



Evidence of Kardar-Parisi-Zhang scaling on a digital quantum simulator

Nathan Keenan^{1,2,3}✉, Niall F. Robertson², Tara Murphy², Sergiy Zhuk² and John Goold^{1,3,4}

Understanding how hydrodynamic behaviour emerges from the unitary evolution of the many-particle Schrödinger equation is a central goal of non-equilibrium statistical mechanics. In this work we implement a digital simulation of the discrete time quantum dynamics of a spin- $\frac{1}{2}$ XXZ spin chain on a noisy near-term quantum device, and we extract the high temperature transport exponent at the isotropic point. We simulate the temporal decay of the relevant spin correlation function at high temperature using a pseudo-random state generated by a random circuit that is specifically tailored to the *ibmq-montreal 27* qubit device. The resulting output is a spin excitation on a homogeneous background on a 21 qubit chain on the device. From the subsequent discrete time dynamics on the device we are able to extract an anomalous super-diffusive exponent consistent with the conjectured Kardar-Parisi-Zhang (KPZ) scaling at the isotropic point. Furthermore we simulate the restoration of spin diffusion with the application of an integrability breaking potential.

npj Quantum Information (2023)9:72; <https://doi.org/10.1038/s41534-023-00742-4>

INTRODUCTION

The idea that quantum dynamics of many-body physics is better simulated by controllable quantum systems was put forward by Richard Feynman 40 years ago¹. This is known as quantum simulation^{2,3} and is expected to be one of the most promising short term goals of near term quantum computing devices⁴ with inevitable applications in diverse areas ranging from quantum chemistry⁵⁻⁷ and material science⁸ to high energy physics⁹. Quantum simulators currently come in two different flavours: analogue and digital¹⁰⁻¹². In an analogue simulator a purpose built controllable quantum many-body system is prepared in the laboratory with the ability to mimic a specific model Hamiltonian of interest. In a digital simulator the quantum dynamics is mapped to a series of discrete time gates that are used to directly manipulate the information encoded in the quantum state².

While analogue simulators are built with a specific model in mind, digital simulation offers the possibility to programme different Hamiltonian models so that a wide range of quantum dynamics is, in principle, accessible on the same device. The possibility of universal simulation of many-body quantum dynamics afforded by digital quantum simulation is a tantalising one. In reality, however, the current devices are still some distance from this goal with noisy gate operations and readout. Ultimately, significant progress in error correcting techniques is needed⁴. In fact it has been on analogue devices where the most significant progress has been made in simulating many-body dynamics¹². However, recent progress in error mitigation techniques for digital devices has brought us closer to getting quantitative results from noisy simulations¹³⁻¹⁵.

One dimensional interacting quantum spin systems are perhaps the simplest non-trivial models used in the field of many-body physics. Despite the obvious shortcomings on noisy near-term quantum devices, there have been several interesting digital simulations¹⁶⁻²⁰ which are restricted to either small systems or short times. These simulations can be viewed as important

benchmarks of device capability. In this work we show how noisy near-term quantum devices can be used to shed important light on a research topic which is at the forefront of research in low-dimensional quantum spin dynamics. The issue we address concerns the nature of the emergent high temperature anomalous hydrodynamics of the spin- $\frac{1}{2}$ XXZ spin chain at the isotropic point²¹.

How macroscopic hydrodynamic behaviour emerges from underlying microscopic physics is a question that has been at the forefront of physics for 200 years^{22,23}. This research continues today in quantum many-body dynamics where the finite temperature transport properties of quantum spin systems is under significant analytical and numerical scrutiny²⁴⁻²⁶. A recent development was the discovery of high-temperature spin super-diffusion at the isotropic point of the spin- $\frac{1}{2}$ XXZ model²⁷ using an open systems approach. In this work the non-equilibrium steady state was found to have a current scaling $\langle J \rangle \propto 1/\sqrt{L}$ consistent with a space time scaling $x \propto t^{1/\nu}$ with $\nu = 3/2$. A numerical study of the infinite temperature spin auto correlation functions at the isotropic point²⁸ has led to the conjecture that the dynamics is in the KPZ universality class²⁹ and further numerical work³⁰ has shown the survival of the associated anomalous scaling of the spin-spin auto-correlation functions at finite temperatures. There is still no clear consensus on the exact conditions for the emergence of this universal behaviour. Integrability is conjectured to be central in the emergence of this scaling and progress in incorporating anomalous diffusion in the context of generalised hydrodynamics^{21,31,32} has been made. The predicted super-diffusive exponent has been observed in a recent experimental study of neutron scattering off $KCuF_3$ which realises an almost ideal XXZ spin chain³³. Furthermore, the scaling was recently confirmed in two analogue simulations of spin chains in both ultra-cold atoms³⁴ and in polariton condensates³⁵.

In this work we perform a digital quantum simulation, of the discrete time dynamics, at the isotropic point of the XXZ model. It

¹Department of Physics, Trinity College Dublin, Dublin 2, Ireland. ²IBM Quantum, IBM Research Europe - Dublin, IBM Technology Campus, Dublin 15, Ireland. ³Trinity Quantum Alliance, Unit 16, Trinity Technology and Enterprise Centre, Pearse Street, D02 YN67 Dublin 2, Ireland. ⁴Algorithmiq Ltd, Kanavakatu 3C 00160, Helsinki, Finland.

✉email: nakeenan@tcd.ie

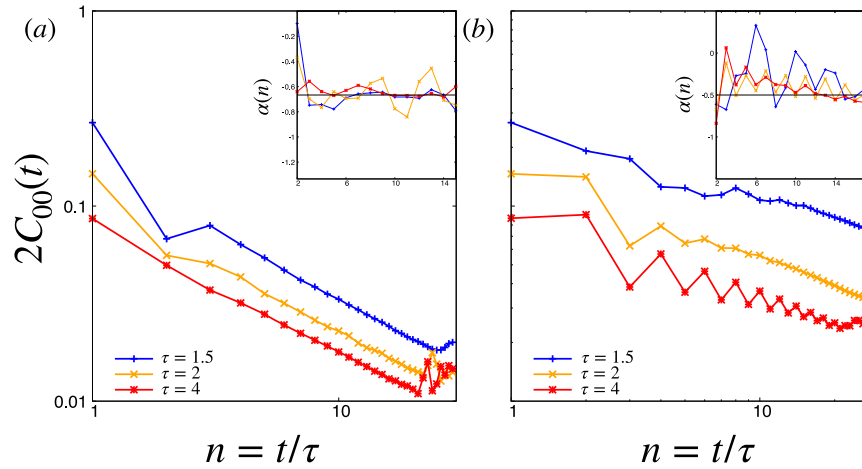


Fig. 1 Classical simulations of scaling dependence on Trotter step. **a** Classical trotter simulations of the spin autocorrelation function on site 0 in the discrete time model for various different timesteps. The inset shows $\alpha(n) = \frac{d \ln C(t)}{d \ln n}$ for the same timesteps, with the black line indicating the expected super-diffusive value $-2/3$. The measured value of α converges towards the expected value of $-2/3$. **b** Classical trotter simulations for the correlator in the discrete time isotropic XXZ model with a staggered field for various time steps. The inset shows $\alpha(n)$ for the same timesteps, with the black line indicating the expected diffusive exponent of $-1/2$. The measured value of α converges towards $-1/2$.

was recently discovered that the Trotterised version of the XXZ model is also integrable³⁶ and the KPZ scaling at the isotropic point remains^{28,37}. This has the distinct advantage on a near term device of being able to simulate for longer times without having to worry about Trotter errors that plague continuous time simulation. We extract the high temperature correlation function following a recent proposal by Richter and Pal^{38,39} that suggests using specially tailored pseudo-random states which are generated from a relatively shallow-depth circuit^{40,41}. The discrete time dynamics of the spin auto-correlation function is then simulated. We apply a zero noise error mitigation strategy (see Supplementary Method 2 for a discussion on this) and remarkably show that the KPZ anomalous exponent can be extracted for over two decades of time evolution. Furthermore we show that the scaling is independent of the time period of the Trotter step and observe the restoration of diffusion, signalled by the emergence of the exponent $\nu=2$, when an integrability breaking staggered field perturbation is applied.

RESULTS

Classical discrete time results

We first demonstrate, using classical simulations⁴², that the transport exponents at the isotropic point for both the (a) clean and (b) staggered field discrete time models are independent of step size. In Fig. 1, we do a first order trotter decomposition of the clean and staggered field models with various timesteps. The power law scaling, in both models, is found to be independent of the time step for the steps chosen. In the insets we show the oscillations of the exponent $\alpha = \frac{d \ln C(t)}{d \ln n}$ around the expected values ($2/3$ for the clean model and $1/2$ for the model with staggered fields) for each model in the insets, where n is the number of Trotter steps. We avoid timesteps near π as the transport behaviour changes drastically due to many-body resonances⁴².

Quantum discrete time results

We now come to the key finding of our work: the digital simulation on a real near term quantum computer. In Fig. 2, we show our results for the spin auto-correlation function simulated on *ibmq-montreal*. We have found that the optimal time-step for our simulations is $\tau = 4J^{-1}$. In (a), we simulate the clean model,

while in (b) we add the staggered field. The green lines show the results on the quantum simulator using a first order Trotter decomposition. Remarkably our results in both the integrable and non-integrable case track the classical simulation well up to two decades in time evolution. This timescale is sufficient to see the emergence of hydrodynamic scaling. The error bars from sampling noise are negligible here compared to the device error, so we omit them. This is the main result of our work.

In order to increase the number of data points for our power law fit we have employed the concept of weaving⁴². This allows us to look at more data points in time. The idea is to artificially increase our time resolution in our study of the the floquet unitary $\mathcal{U}(n\tau)$ ⁴². This is done by adding smaller $\mathcal{U}(\tau' < \tau)$ at the start of the circuit as a modified initial condition, and then weaving the evolution of this new initial state (shifted slightly in time) with the original evolution. We add weaves of $1J^{-1}, 1.5J^{-1}, 2J^{-1}$. Furthermore, in obtaining these results, we employ a form of error mitigation known as ‘zero noise extrapolation’, or zne¹³. However, we do not find that it significantly helps at these time scales for our first order Trotter simulation⁴².

To extract the power law behaviour of the results from the quantum simulations, we analyse the intersection of two regimes in time: (1) Where the power law scaling is present in the classical results, and 2) where the quantum results have little error compared to the classical results. We then fit a power law to the quantum results via least squares. For panel (a) with the clean model, we get that $\alpha \approx -0.644$, and for panel (b) with the staggered external field we get that $\alpha \approx -0.505$. These have relative errors $\sim 3.40\%$ and $\sim 1.00\%$ compared to the expected scalings of $-2/3$ and $-1/2$, respectively.

IBM’s quantum devices are calibrated regularly. When these results were collected, the readout error of qubit 0 was 2.26%, while the average error of all the CNOTs (excluding an outlier at 18.4%) used in the simulation was 1.12%, with a standard deviation of 0.52%.

DISCUSSION

We have provided strong evidence that KPZ scaling and the restoration of diffusion through explicit integrability breaking can be simulated digitally on a near term device. Our work is inspired by the proposal of Richter and Pal³⁸ which exploits a pseudo-random state as a starting point for the simulation (see

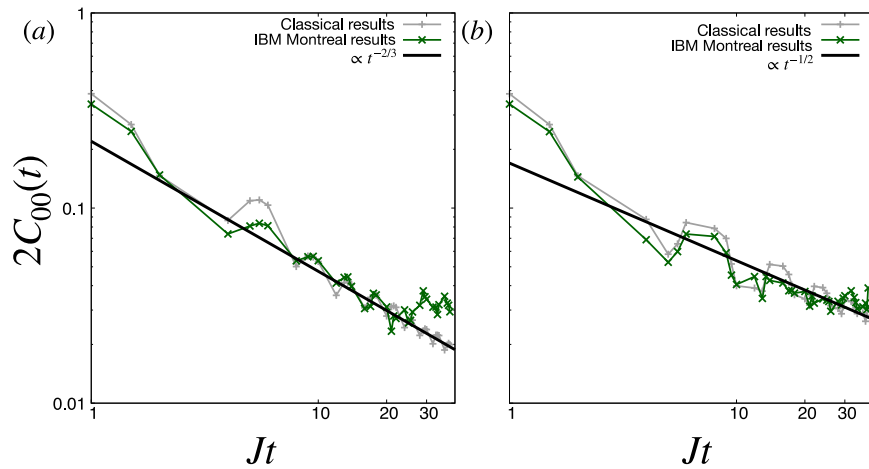


Fig. 2 Comparing the results from the IBM device to the classical simulations. **a** The spin autocorrelation function on site 0 in the discrete time XXZ model at the isotropic point. The trotter step is taken to be $4J^{-1}$, with added weavings from $1J^{-1}$, $1.5J^{-1}$, and $2J^{-1}$. **b** Results for the correlator in the discrete time isotropic XXZ model with a staggered field. The trotter step is taken to be $4J^{-1}$, with added weavings from $1J^{-1}$, $1.5J^{-1}$, and $2J^{-1}$.

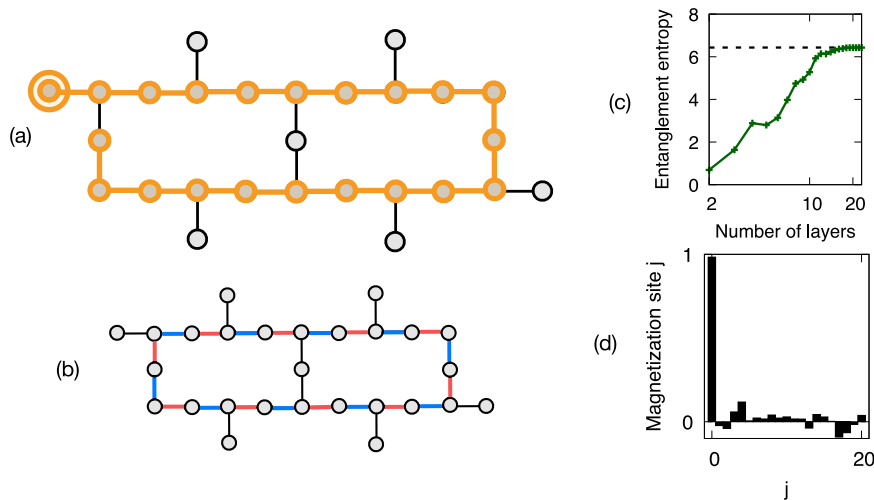


Fig. 3 Mapping our system onto the IBM device, and some properties of the initial state. **a** The *ibmq montreal* qubit connectivity, with a 1-dimensional XXZ model (OBC) mapped onto a 21-qubit chain in the device (we label them q_j). Site q_0 is mapped to the encircled qubit, and is untouched by the randomisation procedure. **b** Red (blue) is CNOT pattern A (B) used in the random state preparation. These are alternated at each layer of the iterated random circuit. **c** The bipartite von Neumann entanglement entropy of the 20 qubit chain as a function of the number of layers in the random circuit. These results are from a clean simulation with connectivity matching that of *ibmq montreal*. The dashed line represents the Page value⁴⁴. **d** The spin density profile of the final state of one sampling of the random circuit.

Supplementary Discussion 2 for a comparison to other methods). It is remarkable that our digital quantum simulation is able to follow closely the classical simulation to over two decades in time evolution. There are several features of this simulation which are worth pointing out. First of all the nature of the initial state appears to be extremely useful for the extraction of infinite temperature transport exponents on current quantum hardware. The precise interplay between noise channels and such pseudotypical states merits future detailed investigations. Since these states are locally equivalent to the identity, it is plausible that they offer a special resilience to unital channels such as dephasing. We have confirmed, on hardware, the suggestion³⁸ that the hydrodynamic scaling is accessible despite inevitable device noise. Secondly and most importantly, the key feature of our simulations is that we work with the discrete time model and this allows us to simulate long times without Trotter error^{28,36}. To our knowledge this is the first extraction of transport exponents of an interacting quantum system on a digital quantum device. Our findings are consistent with recent experiments in a variety of physical

platforms^{33–35,43}. As hardware improves further and the number of good device qubits increase, we hope that our work will inspire further work on high temperature transport of non-integrable and integrable quantum many-body models in regimes not accessible to classical numerics.

METHODS

Initial state preparation

All the quantum simulations in this paper were performed on the *ibmq montreal* 27 qubit device based on coupled transmons. This machine was recently benchmarked to have a quantum volume of 128. The connectivity of the device is shown in Fig. 3a and we will use the 21 qubits which are shown in orange for our dynamical simulations. Our first task, following the suggestion of Richter and Pal³⁸ is to generate a pseudo-random state state on the device leaving all but one qubit untouched (q_0).

The randomisation procedure is split up into two sub-routines; the single qubit gate routine, and the entangling routine. A layer

of the procedure is made up of a single qubit step, followed by an entangling step. The single qubit gate routine is as follows:

1. At layer 1, for each qubit q_j , apply G_j^1 , which is chosen randomly from the set of gates $\{X^{1/2}, Y^{1/2}, T\}$
2. At layer $n > 1$, for each qubit q_j , apply G_j^n , which is chosen randomly from the set $\{X^{1/2}, Y^{1/2}, T\} \setminus G_{n-1}$

Between each single qubit step, we carry out an entangling step. This consists of applying one of two patterns of CX gates across the device. The choice of pattern in alternated between patterns 'A' and 'B' (shown in Fig. 3b) at each step. The randomisation procedure is performed over multiple layers until the state is deemed sufficiently random. The number of layers that are needed is estimated from a classical simulation of the time evolution of the bi-partite entanglement of the random circuit. The results of the classical simulation are shown in Fig. 3c, where we show the half chain von Neumann entropy as a function of the number of layers in our preparation step. We see that already a modest number of layers is enough to saturate the Page value⁴⁴. Figure 3d shows the spin density profile of the final state, on the actual hardware following one sampling of the random circuit. The data was extracted by performing 30,000 shots after one sampling of the circuit.

In this work, we will be interested in performing dynamical quantum simulation of spin spin autocorrelation functions, which take the form

$$C_{jk}(t) = \text{Tr}(S_j^z S_k^z(t)) / 2^L \quad (1)$$

where the trace is over the entire Hilbert space. Following the proposal of Richter and Pal^{38,39}, we will use the output of our state preparation circuit in the evaluation of this object. Let us assume for a moment that the output state of the entire register would be $|\psi_{R,0}\rangle = |0\rangle|\psi_R\rangle$ with $|\psi_R\rangle = \sum_n c_n |n\rangle$, where the expansion is over the entire computational basis. If c_n are Gaussian random numbers with zero mean (i.e the state is drawn randomly from the unitarity invariant Haar measure) then one can approximate the correlation functions by (for details, see ref. ³⁸)

$$C_{jk}(t) = \frac{1}{2} \langle \psi_{R,k} | S_j^z(t) | \psi_{R,k} \rangle + \mathcal{O}(2^{-L/2}). \quad (2)$$

This typicality approach is routinely used to evaluate the time evolution of observables in classical simulations^{24,40,45–48}. Pseudo-random states can be now generated on noisy near-term quantum devices with relatively shallow circuits⁴¹. The state preparation procedure leads to deviations from a Haar random state. However, as argued in refs. ^{38,40} the exact distribution of the coefficients of the states can deviate from Gaussian and still the same result holds⁴⁰. A key finding of ref. ³⁸ is that the state which is output after the initial randomisation phase is robust to modelled device noise. The main purpose of this paper is to use this protocol in order to extract the decay of the spin autocorrelation function on a current quantum hardware.

Discrete time dynamics

The spin- $\frac{1}{2}$ XXZ Hamiltonian which will be the central focus of our simulation is

$$H_{XXZ} = J \sum_{\ell=0}^{L-1} (S_{\ell}^x S_{\ell+1}^x + S_{\ell}^y S_{\ell+1}^y + \Delta S_{\ell}^z S_{\ell+1}^z), \quad (3)$$

where $S_{\ell}^a = \sigma_{\ell}^a / 2$ is the spin operator acting on site ℓ and L is the number of sites. We use open boundary conditions, and focus on the isotropic point ($\Delta = 1$). We define $h_{\ell,\ell+1} = J(S_{\ell}^x S_{\ell+1}^x + S_{\ell}^y S_{\ell+1}^y + \Delta S_{\ell}^z S_{\ell+1}^z)$ and group all of these two-site operators into two sums: $H_1 = \sum_{\ell \text{ odd}} h_{\ell,\ell+1}$, $H_2 = \sum_{\ell \text{ even}} h_{\ell,\ell+1}$. Note that the two-site operators in a given sum all act on disjoint pairs of sites. Therefore all operators commute with all other

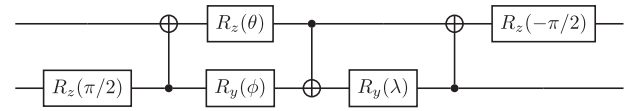


Fig. 4 Implementation of $U_{jk}(\tau)$ on qubits q_j and q_k . Here, $\theta = \Delta\tau / 2 - \pi/2$, and $\phi = \tau/2 - \pi/2$. This circuit equals $U_{jk}(\tau)$ up to a global phase factor of $\exp(-i\pi/4)$.

operators in their respective sums. We now look at the discrete time dynamics given by a Trotter step τ :

$$\begin{aligned} \mathcal{U}(n\tau) &= [\mathcal{U}_{\text{odd}}(\tau)\mathcal{U}_{\text{even}}(\tau)]^n \\ &= \left[\prod_{j=0}^{L/2-1} U_{2j,2j+1}(\tau) \prod_{k=1}^{L/2-1} U_{2k-1,2k}(\tau) \right]^n \end{aligned} \quad (4)$$

where $U_{jk}(\tau) = e^{-iH_{jk}\tau}$. The implementation of $U_{jk}(\tau)$ in a quantum circuit is given by Fig. 4⁴⁹.

Note that if we keep $n\tau$ fixed and take the limit $\tau \rightarrow 0$, we get that $\mathcal{U}(n\tau) \rightarrow e^{-iH_{XXZ}n\tau}$. However, we are less interested in this trotterized unitary as an approximation of the continuous time unitary for the XXZ model, but instead as a floquet system with kicking period τ . This model has Hamiltonian given by:

$$H_{XXZ}^{(\tau)}(t) = H_1 + \tau H_2 \sum_{n \in \mathbb{Z}} \delta(t - n\tau). \quad (5)$$

This Hamiltonian has been shown to also give rise to KPZ like scaling in discrete time^{28,37} and is particularly appealing due to the fact that there is no Trotter error. This was recently exploited in a digital simulation of the spin- $\frac{1}{2}$ XXZ chain in the gapped ($\Delta > 1$) phase on the *ibm kawasaki* 27-qubit machine in order to study the effect of noise on conserved charges⁵⁰. In our simulations we will also be interested in explicitly breaking the integrability of this model by the application of a staggered field which, at high temperatures, is expected to restore diffusion at the isotropic point. To implement this integrability breaking term, we continue like in the previous case, except as well as H_1 and H_2 we add the term $H_3 = \frac{J}{2} \sum_{\ell=0}^{L-1} (-1)^\ell S_{\ell}^z$. The unitary for the discrete time evolution with the staggered field is given by:

$$\mathcal{U}(n\tau) = [\mathcal{U}_{\text{even}}(\tau)\mathcal{U}_3(\tau)\mathcal{U}_{\text{odd}}(\tau)]^n, \quad (6)$$

where $\mathcal{U}_3(\tau) = \prod_j e^{-i\sigma_j^z \theta}$ is implemented as a collection of single qubit rotations. The effective Hamiltonian is now given by

$$H_{\text{stagg}}^{(\tau)}(t) = H_{XXZ}^{(\tau)}(t) + \lim_{\epsilon \rightarrow 0^+} \tau H_3 \sum_{n \in \mathbb{Z}} \delta(t - n\tau + \epsilon), \quad (7)$$

where ϵ is a dummy variable used to ensure we apply the resulting unitaries in the correct order.

DATA AVAILABILITY

Data used in this project are available on request.

CODE AVAILABILITY

Code used for this project is available on request.

Received: 6 April 2023; Accepted: 30 June 2023;

Published online: 20 July 2023

REFERENCES

1. Feynman, R. P. Simulating physics with computers. *Int. J. Theor. Phys.* **21**, 467–488 (1982).
2. Lloyd, S. Universal quantum simulators. *Science* **273**, 1073–1078 (1996).

3. Nielsen, M. A. & Chuang, I. *Quantum Computation and Quantum Information* (American Association of Physics Teachers, 2002).
4. Preskill, J. Quantum computing in the NISQ era and beyond. *Quantum* **2**, 79 (2018).
5. Kassal, I., Whitfield, J. D., Perdomo-Ortiz, A., Yung, Man-Hong & Aspuru-Guzik, Alán Simulating chemistry using quantum computers. *Annu. Rev. Phys. Chem.* **62**, 185–207 (2011).
6. Hastings, M. B., Wecker, D., Bauer, B. & Troyer, M. Improving quantum algorithms for quantum chemistry. *Quantum Inf. Comput.* **15**, 1–21 (2015).
7. Cao, Y. et al. Quantum chemistry in the age of quantum computing. *Chem. Rev.* **119**, 10856–10915 (2019).
8. de Leon, N. P. et al. Materials challenges and opportunities for quantum computing hardware. *Science* **372**, eabb2823 (2021).
9. Nachman, B., Provasoli, D., De Jong, W. A. & Bauer, C. W. Quantum algorithm for high energy physics simulations. *Phys. Rev. Lett.* **126**, 062001 (2021).
10. Georgescu, I. M., Ashhab, S. & Nori, F. Quantum simulation. *Rev. Mod. Phys.* **86**, 153–185 (2014).
11. Tacchino, F., Chiesa, A., Carretta, S. & Gerace, D. Quantum computers as universal quantum simulators: state-of-the-art and perspectives. *Adv. Quantum Technol.* **3**, 1900052 (2020).
12. Daley, A. J. et al. Practical quantum advantage in quantum simulation. *Nature* **607**, 667–676 (2022).
13. Temme, K., Bravyi, S. & Gambetta, J. M. Error mitigation for short-depth quantum circuits. *Phys. Rev. Lett.* **119**, 180509 (2017).
14. Endo, S., Benjamin, S. C. & Li, Y. Practical quantum error mitigation for near-future applications. *Phys. Rev. X* **8**, 031027 (2018).
15. Kim, Y. et al. Scalable error mitigation for noisy quantum circuits produces competitive expectation values. *Nat. Phys.* **19**, 1–8 (2023).
16. Zhukov, A. A., Remizov, S. V., Pogosov, W. V. & Lozovik, Y. E. Algorithmic simulation of far-from-equilibrium dynamics using quantum computer. *Quantum Inf.* **17**, 1–26 (2018).
17. Cervera-Lierta, A. Exact Ising model simulation on a quantum computer. *Quantum* **2**, 114 (2018).
18. Francis, A., Freericks, J. K. & Kemper, A. F. Quantum computation of magnon spectra. *Phys. Rev. B* **101**, 014411 (2020).
19. Smith, A., Kim, M. S., Pollmann, F. & Knolle, J. Simulating quantum many-body dynamics on a current digital quantum computer. *Npj Quantum Inf.* **5**, 106 (2019).
20. Vovrosh, J. & Knolle, J. Confinement and entanglement dynamics on a digital quantum computer. *Sci. Rep.* **11**, 11577 (2021).
21. Bulchandani, V. B., Gopalakrishnan, S. & Ilievski, E. Superdiffusion in spin chains. *J. Stat. Mech. Theory Exp.* **2021**, 084001 (2021).
22. Fourier, J. B. *Théorie Analytique de la Chaleur* (Gauthier-Villars et fils, 1822).
23. Buchanan, M. Heated debate in different dimensions. *Nat. Phys.* **1**, 71–71 (2005).
24. Bertini, B. et al. Finite-temperature transport in one-dimensional quantum lattice models. *Rev. Mod. Phys.* **93**, 025003 (2021).
25. Bohrdt, A., Mendl, C. B., Endres, M. & Knap, M. Scrambling and thermalization in a diffusive quantum many-body system. *N. J. Phys.* **19**, 063001 (2017).
26. Rakovszky, T., Pollmann, F. & Von Keyserlingk, C. W. Diffusive hydrodynamics of out-of-time-ordered correlators with charge conservation. *Phys. Rev. X* **8**, 031058 (2018).
27. Žnidarič, M. Spin transport in a one-dimensional anisotropic Heisenberg model. *Phys. Rev. Lett.* **106**, 220601 (2011).
28. Ljubotina, M., Žnidarič, M. & Prosen, T. Kardar-Parisi-Zhang physics in the quantum heisenberg magnet. *Phys. Rev. Lett.* **122**, 210602 (2019).
29. Kardar, M., Parisi, G. & Zhang, Yi-Cheng Dynamic scaling of growing interfaces. *Phys. Rev. Lett.* **56**, 889–892 (1986).
30. Dupont, M., Sherman, N. E. & Moore, J. E. Spatiotemporal crossover between low- and high-temperature dynamical regimes in the quantum heisenberg magnet. *Phys. Rev. Lett.* **127**, 107201 (2021).
31. Ilievski, E., De Nardis, J., Gopalakrishnan, S., Vasseur, R. & Ware, B. Super-universality of superdiffusion. *Phys. Rev. X* **11**, 031023 (2021).
32. Gopalakrishnan, S. & Vasseur, R. Anomalous transport from hot quasiparticles in interacting spin chains. *Rep. Prog. Phys.* **86**, 036502 (2022).
33. Scheie, A. et al. Detection of Kardar-Parisi-Zhang hydrodynamics in a quantum heisenberg spin-1/2 chain. *Nat. Phys.* **17**, 726–730 (2021).
34. Wei, D. et al. Quantum gas microscopy of Kardar-Parisi-Zhang superdiffusion. *Science* **376**, 716–720 (2022).
35. Fontaine, Q. et al. Kardar-Parisi-Zhang universality in a one-dimensional polariton condensate. *Nature* **608**, 687 (2022).
36. Vanicat, M., Zadnik, L. & Prosen, T. Integrable trotterization: local conservation laws and boundary driving. *Phys. Rev. Lett.* **121**, 030606 (2018).
37. Krajnik, Žiga & Prosen, T. Kardar-Parisi-Zhang physics in integrable rotationally symmetric dynamics on discrete space-time lattice. *J. Stat. Phys.* **179**, 110–130 (2020).
38. Richter, J. & Pal, A. Simulating hydrodynamics on noisy intermediate-scale quantum devices with random circuits. *Phys. Rev. Lett.* **126**, 230501 (2021).
39. Lunt, O., Richter, J. & Pal, A. In *Entanglement in Spin Chains: From Theory to Quantum Technology Applications* 251–284 (Springer Nature, 2022).
40. Jin, F. et al. Random state technology. *J. Phys. Soc. Jpn.* **90**, 012001 (2021).
41. Arute, F. et al. Quantum supremacy using a programmable superconducting processor. *Nature* **574**, 505–510 (2019).
42. Geller, M. R. et al. Quantum simulation of operator spreading in the chaotic Ising model. *Phys. Rev. E* **105**, 035302 (2022).
43. Joshi, M. K. et al. Observing emergent hydrodynamics in a long-range quantum magnet. *Science* **376**, 720–724 (2022).
44. Page, D. N. Information in black hole radiation. *Phys. Rev. Lett.* **71**, 3743–3746 (1993).
45. Steinigeweg, R., Gemmer, J. & Brenig, W. Spin-current autocorrelations from single pure-state propagation. *Phys. Rev. Lett.* **112**, 120601 (2014).
46. Richter, J. et al. Magnetization and energy dynamics in spin ladders: evidence of diffusion in time, frequency, position, and momentum. *Phys. Rev. B* **99**, 144422 (2019).
47. Richter, J. *Quantum Many-Body Dynamics of Isolated Systems Close to and Far Away From Equilibrium*. Thesis, Universität Osnabrück (2020).
48. Chiaracane, C., Pietracaprina, F., Purkayastha, A. & Goold, J. Quantum dynamics in the interacting Fibonacci chain. *Phys. Rev. B* **103**, 184205 (2021).
49. Vatan, F. & Williams, C. Optimal quantum circuits for general two-qubit gates. *Phys. Rev. A* **69**, 032315 (2004).
50. Maruyoshi, K. et al. Conserved charges in the quantum simulation of integrable spin chains. *J. Phys. A Math. Theor.* **56**, 165301 (2023).

ACKNOWLEDGEMENTS

We thank the QuSys group at TCD, A. Purkayastha and A. Silva for useful discussions. J.G. is funded by a Science Foundation Ireland-Royal Society University Research Fellowship, the European Research Council Starting Grant ODYSSEY (Grant Agreement No. 758403). This project was made possible through the TCD-IBM predoctoral programme.

AUTHOR CONTRIBUTIONS

N.K.: investigation, methodology, software, validation, formal analysis, visualisation, writing (original draft), writing (review and editing); N.F.R.: investigation, writing (review and editing); T.M.: investigation; S.Z.: supervision, writing (review and editing); J.G.: conceptualisation, supervision, resources, writing (original draft), writing (review and editing).

COMPETING INTERESTS

The authors declare no competing interests.

ADDITIONAL INFORMATION

Supplementary information The online version contains supplementary material available at <https://doi.org/10.1038/s41534-023-00742-4>.

Correspondence and requests for materials should be addressed to Nathan Keenan.

Reprints and permission information is available at <http://www.nature.com/reprints>

Publisher's note Springer Nature remains neutral with regard to jurisdictional claims in published maps and institutional affiliations.



Open Access This article is licensed under a Creative Commons Attribution 4.0 International License, which permits use, sharing, adaptation, distribution and reproduction in any medium or format, as long as you give appropriate credit to the original author(s) and the source, provide a link to the Creative Commons license, and indicate if changes were made. The images or other third party material in this article are included in the article's Creative Commons license, unless indicated otherwise in a credit line to the material. If material is not included in the article's Creative Commons license and your intended use is not permitted by statutory regulation or exceeds the permitted use, you will need to obtain permission directly from the copyright holder. To view a copy of this license, visit <http://creativecommons.org/licenses/by/4.0/>.